Mon. Not. R. Astron. Soc. **372,** 1315–1324 (2006) doi:10.1111/j.1365-2966.2006.10937.x

Photometric and spectroscopic evolution of the Type IIP supernova SN 2004et

D. K. Sahu,★ G. C. Anupama,★ S. Srividya and S. Muneer
Indian Institute of Astrophysics, Koramangala, Bangalore 560 034, India

Accepted 2006 August 14. Received 2006 August 11; in original form 2006 May 15

ABSTRACT

We present optical photometry and spectroscopy of the Type IIP supernova SN 2004et that occurred in the nearby galaxy NGC 6946. The observations span a time range of 8–541 d after explosion. The late time bolometric luminosity and the Hα luminosity in the nebular phase indicate that $0.06 \pm 0.02\,M_\odot$ of ^{56}Ni was synthesized during the explosion. The plateau luminosity, its duration and the expansion velocity of the supernova at the middle of the plateau indicate an explosion energy of $E_{\rm exp} = 1.20^{+0.38}_{-0.30} \times 10^{51}$ erg. The late time light curve and the evolution of the [O I] and Hα emission-line profiles indicate the possibility of an early dust formation in the supernova ejecta. The luminosity of [O I] 6300, 6364 Å doublet, before the dust formation phase, is found to be comparable to that of SN 1987A at similar epochs, implying an oxygen mass in the range 1.5–2 $M_\odot$, and a main-sequence mass of 20 $M_\odot$ for the progenitor.

Key words: supernovae: general – supernovae: individual: SN 2004et – galaxies: individual: NGC 6946

1 INTRODUCTION

Supernovae have been classified mainly based on their spectrum near maximum, the events which show the presence of hydrogen lines have been termed as supernovae Type II (SNe II) and those which do not show hydrogen are classified as Type I. Type II events are thought to arise from the gravitational collapse of stars more massive than 8 $M_\odot$. SNe II have been further divided based on their light curve (Baron, Ciatti & Rosino 1979) as Type IIL (linear) and Type IIP (plateau). Supernovae Type IIP (SNe IIP) are characterized by a plateau of nearly constant luminosity in their light curve, originating because of propagation of a cooling and recombination wave through the supernova envelope.

Hamuy (2003) has shown that SNe IIP form a sequence from low-luminosity, low-velocity, nickel-poor events to bright, high-velocity, nickel-rich objects. Further, there is an indication that more massive progenitors produce more energetic explosion, and supernovae with greater energies produce more nickel. The direct identification of the progenitor of a few SNe IIP indicates that these events arise from stars with masses in the range ∼8–15 $M_\odot$ (Van Dyk, Li & Filippenko 2003; Smartt et al. 2004; Li et al. 2006).

SN 2004et was discovered by Moretti on 2004 September 27, in the nearby starburst galaxy NGC 6946, which has already produced seven supernovae during 1917–2003. Based on a high-resolution spectrum that showed a relatively featureless spectrum with a very broad, low-contrast Hα emission, Zwitter, Munari & Moretti (2004) classified the supernova as a Type II event, which was later confirmed by a low-resolution spectrum taken on 2004 October 01 by Filippenko et al. (2004). The P Cygni profile of Hα was greatly dominated by the emission component, while the other hydrogen Balmer lines had a more typical P Cygni profile. The continuum was quite blue, although there was very low flux shortwards of 4000Å. The supernova was detected in the radio frequencies at 22.460 and 8.460 GHz on 2004 October 5.128 (Stockdale et al. 2004), suggesting the presence of appreciable circumstellar material around SN 2004et. Based on pre-explosion images of NGC 6946, Li et al. (2005b) identified the candidate progenitor as a yellow supergiant with an estimated zero-age main-sequence mass of $15^{+5}_{-2}\,M_\odot$. The identification of the progenitor was confirmed with post-outburst *Hubble Space Telescope* images obtained on 2005 May 02 (Li, Filippenko & Van Dyk 2005a). This makes SN 2004et one of the few core-collapse supernovae with a directly identified progenitor.

The proximity and brightness of SN 2004et made it an ideal target for an intensive monitoring. In this paper, we present the results based on extensive photometric and spectroscopic observations of SN 2004et during ∼8–541 d since explosion.

2 OBSERVATIONS AND DATA REDUCTION

2.1 Photometry

SN 2004et was observed with the 2-m Himalayan Chandra Telescope (HCT) of the Indian Astronomical Observatory (IAO), Hanle, India, using the Himalaya Faint Object Spectrograph Camera (HFOSC), equipped with a 2048 × 4096 pixel^2 CCD. The central 2048 × 2048 region of the CCD used for imaging covers a field

★E-mail: dks@crest.ernet.in (DKS); gca@iiap.res.in (GCA)

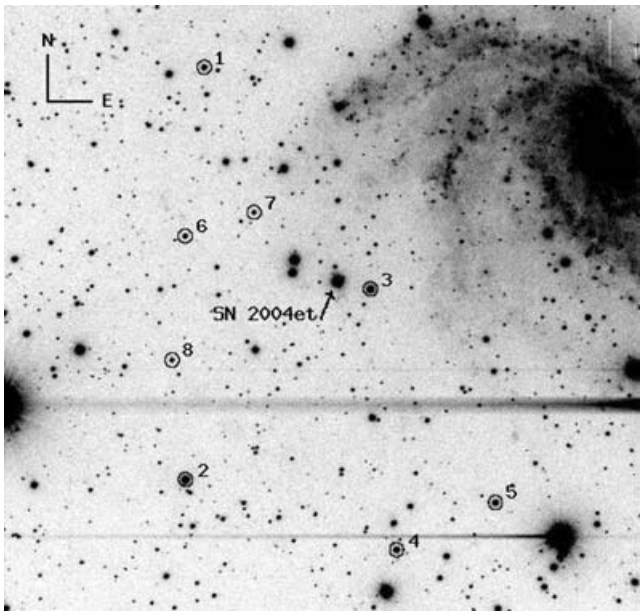

Figure 1. Identification chart for SN 2004et. The stars used as local standards are marked as numbers 1–8. The field of view is 10 × 10 arcmin^2.

of view of 10 × 10 arcmin^2, with a scale of 0.296 arcsec pixel^{-1}. The photometric monitoring of SN 2004et, in Bessell *UBVRI* filters (Bessell 1990), began on 2004 September 29, soon after its discovery, and continued until 2006 March 16.

The data were bias-subtracted, flat-field corrected and cosmic rays removed adopting the standard manner, using the various tasks available under the IRAF software. Data obtained on photometric nights were calibrated using standard fields (Landolt 1992), and a sequence of local standards in the supernova field (Fig. 1) was used for photometric calibration of the supernova. Table 1 gives the *U*, *B*, *V*, *R*, *I* magnitudes of the secondary standards averaged over a few photometric nights.

Aperture photometry was performed on the local standards using an aperture of radius determined based on an aperture growth curve. The magnitudes of the supernova and also the local standards were estimated using the profile-fitting method, using a fitting radius corresponding to the full width at half maximum of the stellar profile. The difference between aperture and profile-fitting magnitudes was obtained using the standards, and this correction was applied to the supernova magnitude. The supernova magnitudes were calibrated differentially with respect to the local standards listed in Table 1. The final magnitude of the supernova was derived by taking an average of these estimates. The estimated supernova magnitudes and errors are listed in Table 2. The errors in the magnitudes were estimated by combining the fit errors in quadrature with those introduced by the transformation of instrumental magnitudes into the standard system.

2.2 Spectroscopy

The spectroscopic observations of SN 2004et started on 2004 October 16 and continued until 2005 December 30, corresponding to ∼25 to ∼465 d after explosion. The journal of observations are given in Table 3. All spectra were obtained in the wavelength range 3500–7000 and 5200–9200 Å at a spectral resolution of ∼7 Å. A few spectra, in the wavelength range 4000–8500 Å, were also obtained with the 1-m telescope at the Vainu Bappu Observatory, Kavalur, India, using the Universal Astronomical Grating (UAG) spectrograph. All data were reduced using the standard routines within IRAF. The data were bias-corrected, flat-fielded, and the one-dimensional spectra were extracted using the optimal extraction method. The wavelength calibration was done using FeAr and FeNe lamp spectra. The instrumental response curves were obtained using spectrophotometric standards observed on the same night, and the supernova spectra were brought to a relative flux scale. On a few nights when the spectrophotometric standards were not observed, the response curves obtained on other nights were used for the flux calibration. The flux-calibrated spectra in the two different regions were combined to a weighted mean to give the final spectrum on a relative flux scale. The spectra were brought to an absolute flux scale using zero points obtained by comparing with the photometric magnitudes. The telluric lines are not removed from the spectra.

2.3 Light curve

The light curves of SN 2004et in the *UBVRI* bands are plotted in Fig. 2. Based on the non-detection of the supernova, with a limiting magnitude of 19.4 ± 1.2, on September 22.017 and the subsequent detection at a magnitude of 15.17 ± 0.16 on September 22.983, Li et al. (2005b) constrained the date of explosion to be 2004 September 22.0 (JD 245 3270.5). Our photometric observations of SN 2004et thus span the range of 8 d (JD 245 3278.2) to 541 d (JD 245 3811.4) since explosion.

A family of cubic spline fits was made to the observed data points around maximum to estimate the date of maximum and maximum magnitude. The dates of maximum and maximum magnitudes were determined as an average of the values of these fits with the uncertainties given by the respective standard deviation of the estimates. The values thus obtained are $m_U(\max) = 12.17 \pm 0.05$ on JD 245 3279.93 ± 1.50, $m_B(\max) = 12.89 \pm 0.02$ on JD 245 3280.90 ± 2.13, $m_V(\max) = 12.55 \pm 0.01$ on JD 245 3286.58 ± 0.50,

Table 1. Magnitudes for the sequence of secondary standard stars in the field of SN 2004et. The stars are identified in Fig. 1.

ID	*U*	*B*	*V*	*R*	*I*
1	15.927 ± 0.020	15.828 ± 0.008	15.130 ± 0.009	14.672 ± 0.009	14.219 ± 0.009
2	14.439 ± 0.027	14.415 ± 0.010	13.773 ± 0.009	13.353 ± 0.007	12.936 ± 0.011
3	16.665 ± 0.021	15.521 ± 0.010	14.265 ± 0.008	13.568 ± 0.011	12.903 ± 0.008
4	15.840 ± 0.024	15.544 ± 0.017	14.726 ± 0.016	14.255 ± 0.016	13.802 ± 0.009
5	15.780 ± 0.021	15.582 ± 0.012	14.795 ± 0.011	14.336 ± 0.007	13.854 ± 0.008
6	17.485 ± 0.033	16.910 ± 0.012	15.953 ± 0.012	15.399 ± 0.012	14.866 ± 0.009
7	16.957 ± 0.028	16.827 ± 0.015	16.202 ± 0.011	15.782 ± 0.015	15.365 ± 0.025
8	16.865 ± 0.034	16.870 ± 0.017	16.233 ± 0.011	15.842 ± 0.015	15.422 ± 0.015

Table 2. Photometric observations of SN 2004et.

Date	JD 245 3000+	Phase[a] (d)	*U*	*B*	*V*	*R*	*I*
2004/09/29	278.202	7.70	12.308 ± 0.035	12.900 ± 0.018	12.650 ± 0.013	12.360 ± 0.021	
2004/09/30	279.225	8.73	12.224 ± 0.034	12.932 ± 0.026	12.633 ± 0.021	12.331 ± 0.012	
2004/10/01	280.200	9.70	12.254 ± 0.034	12.907 ± 0.017	12.629 ± 0.016	12.314 ± 0.013	
2004/10/06	285.118	14.62	12.418 ± 0.032	12.908 ± 0.012	12.556 ± 0.012	12.216 ± 0.014	12.019 ± 0.018
2004/10/07	286.065	15.57	12.514 ± 0.035	12.921 ± 0.016	12.547 ± 0.013	12.200 ± 0.026	12.009 ± 0.014
2004/10/09	288.059	17.56	12.563 ± 0.038	12.963 ± 0.016	12.549 ± 0.022	12.182 ± 0.018	11.962 ± 0.014
2004/10/11	290.060	19.56	12.673 ± 0.034	12.998 ± 0.017	12.552 ± 0.011	12.156 ± 0.019	11.937 ± 0.019
2004/10/12	291.237	20.74	12.751 ± 0.035	13.047 ± 0.012	12.560 ± 0.019	12.167 ± 0.014	11.927 ± 0.024
2004/10/13	292.077	21.58	12.793 ± 0.033	13.065 ± 0.017	12.558 ± 0.013	12.161 ± 0.020	11.923 ± 0.022
2004/10/14	293.103	22.60	12.885 ± 0.037	13.113 ± 0.021	12.560 ± 0.024	12.160 ± 0.017	11.918 ± 0.019
2004/10/15	294.114	23.61	12.997 ± 0.035	13.162 ± 0.009	12.557 ± 0.019	12.154 ± 0.020	11.922 ± 0.012
2004/10/16	295.125	24.62	13.063 ± 0.046	13.203 ± 0.017	12.568 ± 0.023	12.156 ± 0.015	11.912 ± 0.021
2004/10/17	296.066	25.57	13.178 ± 0.042	13.240 ± 0.013	12.572 ± 0.014	12.157 ± 0.016	11.892 ± 0.018
2004/10/22	301.046	30.55	13.638 ± 0.046	13.501 ± 0.028	12.656 ± 0.020	12.210 ± 0.007	11.916 ± 0.016
2004/10/23	302.045	31.55	13.737 ± 0.043	13.573 ± 0.021	12.646 ± 0.023	12.207 ± 0.021	11.922 ± 0.013
2004/10/26	305.083	34.58	13.865 ± 0.048	13.694 ± 0.026	12.704 ± 0.016	12.249 ± 0.020	11.936 ± 0.019
2004/10/27	306.055	35.55		13.740 ± 0.041	12.687 ± 0.022	12.231 ± 0.020	11.914 ± 0.027
2004/10/29	308.218	37.72	14.195 ± 0.036	13.846 ± 0.027	12.746 ± 0.017	12.247 ± 0.016	11.923 ± 0.021
2004/10/30	309.125	38.62	14.268 ± 0.050	13.867 ± 0.013	12.755 ± 0.023	12.248 ± 0.022	11.929 ± 0.020
2004/11/01	311.132	40.63	14.385 ± 0.033	13.930 ± 0.018	12.767 ± 0.019	12.264 ± 0.008	11.928 ± 0.016
2004/11/05	315.053	44.55	14.623 ± 0.035	14.046 ± 0.019	12.802 ± 0.016	12.283 ± 0.023	11.953 ± 0.031
2004/11/11	321.034	50.53	14.903 ± 0.039	14.197 ± 0.018	12.862 ± 0.029	12.282 ± 0.020	11.934 ± 0.039
2004/11/12	322.067	51.57	14.991 ± 0.034	14.227 ± 0.013	12.848 ± 0.022	12.294 ± 0.016	11.934 ± 0.020
2004/11/16	326.046	55.55	15.180 ± 0.038	14.329 ± 0.016	12.884 ± 0.018	12.310 ± 0.017	11.930 ± 0.014
2004/11/20	330.070	59.57	15.347 ± 0.041	14.408 ± 0.024	12.910 ± 0.023	12.301 ± 0.019	11.927 ± 0.021
2004/11/24	334.072	63.57	15.533 ± 0.041	14.486 ± 0.026	12.942 ± 0.022	12.321 ± 0.022	11.946 ± 0.015
2004/11/25	335.035	64.54	15.568 ± 0.040	14.499 ± 0.024	12.930 ± 0.028	12.317 ± 0.025	11.920 ± 0.019
2004/12/04	344.063	73.56	15.861 ± 0.026	14.657 ± 0.016	12.994 ± 0.024	12.352 ± 0.020	11.946 ± 0.011
2004/12/08	348.041	77.54		14.726 ± 0.013	13.024 ± 0.014	12.371 ± 0.013	11.944 ± 0.019
2004/12/12	352.034	81.53	16.160 ± 0.034	14.788 ± 0.020	13.031 ± 0.013	12.372 ± 0.020	11.957 ± 0.026
2004/12/16	356.096	85.60	16.291 ± 0.034	14.851 ± 0.012	13.075 ± 0.016	12.408 ± 0.018	11.978 ± 0.020
2004/12/29	369.038	98.54		15.118 ± 0.012	13.247 ± 0.024	12.524 ± 0.026	12.093 ± 0.038
2005/01/06	377.044	106.54		15.346 ± 0.011	13.405 ± 0.020	12.651 ± 0.014	12.197 ± 0.022
2005/01/10	381.044	110.54	17.221 ± 0.035	15.522 ± 0.008	13.535 ± 0.013	12.776 ± 0.013	12.296 ± 0.011
2005/01/13	384.043	113.54	17.524 ± 0.040	15.665 ± 0.031	13.660 ± 0.021	12.843 ± 0.022	12.374 ± 0.027
2005/01/23	394.041	123.54		16.527 ± 0.193	14.488 ± 0.117	13.561 ± 0.114	13.005 ± 0.030
2005/03/07	436.511	166.01		17.736 ± 0.069	15.822 ± 0.016	14.735 ± 0.021	14.154 ± 0.019
2005/03/24	454.490	183.99		17.863 ± 0.034	16.002 ± 0.024	14.891 ± 0.022	14.349 ± 0.017
2005/04/01	462.484	191.98			16.117 ± 0.027	14.990 ± 0.012	14.417 ± 0.019
2005/04/10	471.473	200.97				15.048 ± 0.027	
2005/04/13	474.472	203.97		17.961 ± 0.032	16.199 ± 0.013	15.075 ± 0.014	14.527 ± 0.013
2005/04/15	476.469	205.97		17.997 ± 0.037	16.230 ± 0.027	15.102 ± 0.020	14.548 ± 0.020
2005/04/21	482.403	211.90		18.019 ± 0.035	16.290 ± 0.017	15.152 ± 0.015	14.608 ± 0.020
2005/05/06	497.392	226.89		18.093 ± 0.009	16.436 ± 0.008	15.314 ± 0.009	14.763 ± 0.019
2005/05/27	518.448	247.95		18.260 ± 0.037	16.662 ± 0.023	15.551 ± 0.018	15.016 ± 0.016
2005/05/28	519.385	248.89		18.250 ± 0.018	16.659 ± 0.009	15.538 ± 0.015	15.024 ± 0.021
2005/06/01	523.393	252.89		18.279 ± 0.019	16.705 ± 0.012	15.575 ± 0.009	15.072 ± 0.014
2005/06/07	529.402	258.90		18.322 ± 0.017	16.773 ± 0.012	15.652 ± 0.008	15.127 ± 0.013
2005/06/20	542.419	271.92		18.389 ± 0.019	16.912 ± 0.008	15.792 ± 0.011	15.257 ± 0.016
2005/06/24	546.410	275.91	19.553 ± 0.055	18.414 ± 0.017	16.957 ± 0.017	15.832 ± 0.014	15.336 ± 0.011
2005/06/25	547.418	276.92	19.491 ± 0.055	18.453 ± 0.027	16.975 ± 0.017	15.852 ± 0.016	15.363 ± 0.013
2005/07/09	561.414	290.91	19.630 ± 0.048	18.552 ± 0.020	17.127 ± 0.027	16.018 ± 0.015	15.538 ± 0.012
2005/07/19	571.406	300.91		18.600 ± 0.017	17.245 ± 0.018	16.140 ± 0.013	15.666 ± 0.019
2005/07/23	575.267	304.77	19.526 ± 0.054	18.615 ± 0.018	17.284 ± 0.010	16.183 ± 0.015	15.707 ± 0.020
2005/08/01	584.290	313.79			17.371 ± 0.036	16.298 ± 0.008	15.856 ± 0.016
2005/08/07	590.250	319.75		18.743 ± 0.018	17.446 ± 0.014	16.363 ± 0.014	15.921 ± 0.011
2005/08/17	600.298	329.80		18.836 ± 0.019	17.571 ± 0.014	16.481 ± 0.015	16.059 ± 0.016
2005/08/23	606.235	335.73		18.902 ± 0.023	17.638 ± 0.019	16.563 ± 0.012	16.125 ± 0.016
2005/09/10	624.223	353.72		19.024 ± 0.019	17.831 ± 0.013	16.789 ± 0.011	16.371 ± 0.009
2005/09/28	642.095	371.59	19.982 ± 0.034	19.187 ± 0.018	18.044 ± 0.017	17.024 ± 0.013	16.647 ± 0.020
2005/09/30	644.133	373.63	19.905 ± 0.032	19.182 ± 0.015	18.067 ± 0.009	17.065 ± 0.007	16.667 ± 0.010
2005/10/17	661.207	390.71		19.278 ± 0.078	18.264 ± 0.018	17.254 ± 0.018	16.874 ± 0.027

Table 2 – *continued*

Date	JD 245 3000+	Phase[a] (d)	*U*	*B*	*V*	*R*	*I*
2005/10/27	671.175	400.67		19.422 ± 0.015	18.376 ± 0.010	17.403 ± 0.012	17.036 ± 0.014
2005/11/23	698.109	427.61		19.680 ± 0.017	18.730 ± 0.016	17.798 ± 0.006	17.426 ± 0.017
2005/12/26	731.103	460.60			19.202 ± 0.016	18.318 ± 0.013	17.919 ± 0.025
2006/03/06	801.493	531.29				19.477 ± 0.027	
2006/03/16	811.426	540.93			20.348 ± 0.041	19.608 ± 0.0265	

[a]Relative to the epoch of explosion (JD 245 3270.5).

Table 3. Journal of spectroscopic observations of SN 2004et.

Date	JD 245 3000+	Phase[a] (d)	Range (Å)
2004/10/16	295.1	24.60	3500–7000; 5200–9200
2004/10/22	301.1	30.60	3500–7000; 5200–9200
2004/10/27	306.0	35.50	5200–9200
2004/10/30	309.1	38.60	3500–7000; 5200–9200
2004/11/01	311.2	40.70	3500–7000; 5200–9200
2004/11/11	321.0	50.50	3500–7000; 5200–9200
2004/11/16	326.1	55.60	3500–7000; 5200–9200
2004/11/18	328.1	57.50	4000–8500[b]
2004/11/19	329.2	58.60	4000–8500[b]
2004/11/24	334.0	63.50	3500–7000; 5200–9200
2004/12/04	344.1	73.60	3500–7000; 5200–9200
2004/12/14	354.0	83.50	3500–7000; 5200–9200
2004/12/17	357.0	86.50	3500–7000; 5200–9200
2004/12/29	369.1	98.60	3500–7000; 5200–9200
2005/01/12	383.1	112.60	3500–7000; 5200–9200
2005/03/03	433.5	163.00	3500–7000; 5200–9200
2005/03/13	443.5	173.00	3500–7000; 5200–9200
2005/03/25	455.4	184.90	3500–7000; 5200–9200
2005/04/10	471.4	200.90	3500–7000; 5200–9200
2005/04/21	482.4	211.90	3500–7000; 5200–9200
2005/05/06	497.4	226.90	3500–7000; 5200–9200
2005/05/28	516.3	245.80	3500–7000; 5200–9200
2005/06/01	523.4	252.90	3500–7000; 5200–9200
2005/06/07	529.4	258.90	3500–7000; 5200–9200
2005/06/25	547.4	276.90	3500–7000; 5200–9200
2005/07/19	571.4	300.90	3500–7000; 5200–9200
2005/08/01	584.3	313.80	3500–7000; 5200–9200
2005/10/17	661.2	390.70	3500–7000; 5200–9200
2005/10/27	671.1	400.60	3500–7000; 5200–9200
2005/11/23	598.1	427.60	3500–7000; 5200–9200
2005/12/30	735.1	464.60	3500–7000; 5200–9200

[a]Relative to the epoch of explosion (JD 245 3270.5).
[b]Observed from Vainu Bappu Observatory, Kavalur.

$m_R(\max) = 12.15 \pm 0.02$ on JD 245 3291.47 ± 1.81 and $m_I(\max) = 11.91 \pm 0.03$ on JD 245 3294.57 ± 1.37. The *B* maximum occurred ∼10 d after the explosion.

The light curves in the *UBVRI* bands show an initial rise, followed by a plateau in the *VRI* bands, which extends up to ∼110 d from the date of explosion. The plateau in the *VRI* light curves and a decline rate of $\beta^B_{100} = 2.2$ mag in the *B* light curve over the first 100 d since maximum light establish that SN 2004et is a Type IIP event, since the decline rate for SNe IIP is $\beta^B_{100} < 3.5$ (Patat et al. 1994). After the initial rise to maximum, the *U*-band light curve declines rapidly till ∼100 d, while the decline in the *B* band is less steep compared to that of the *U* band. The *V*-band light curve shows a slowly declining trend in the plateau phase while the light curve in the *R* and *I* bands shows a nearly constant brightness during the plateau phase.

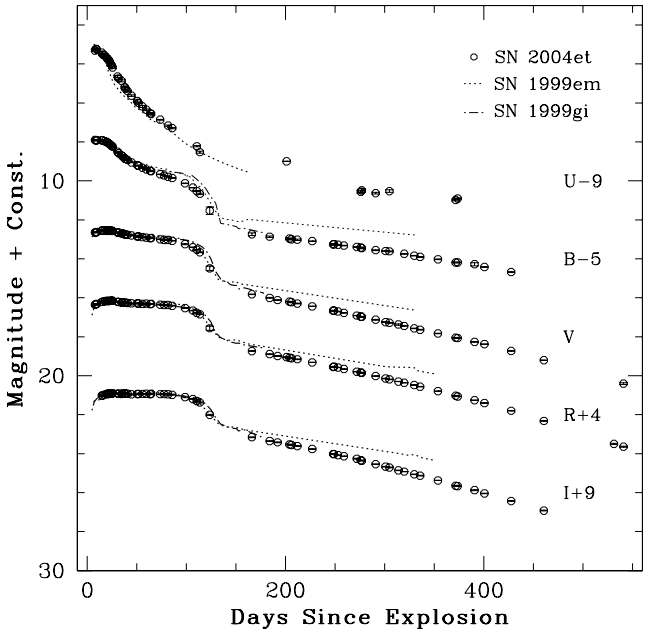

Figure 2. *UBVRI* light curve of SN 2004et plotted with other Type IIP SNe. Light curves of SN 2004et have been shifted by the reported amounts, other light curves have been shifted by arbitrary amounts to match those of SN 2004et.

Following the plateau phase, the *V* light curve displays a steep decline of ∼2 mag in ∼40 d (day ∼110 to ∼150; JD 245 3380 to JD 245 3420). Subsequently, the decline is linear in all the bands, with decline rates of $\gamma_B \sim 0.64$, $\gamma_V \sim 1.04$, $\gamma_R \sim 1.01$ and $\gamma_I \sim 1.07$, from ∼180 to ∼310 d after explosion. The decline rate steepens beyond 310 d to $\gamma_B \sim 0.84$, $\gamma_V \sim 1.21$, $\gamma_R \sim 1.31$ and $\gamma_I \sim 1.39$. The photometric evolution of SNe IIP at late phases is powered by radioactive decay of ^{56}Co into ^{56}Fe, and the expected decay rate is $\gamma = 0.98$ mag $(100\,\mathrm{d})^{-1}$, especially in the *V* band (Patat et al. 1994). Except for the *B* band, the decay rates obtained during the early nebular phase (180–310 d) are close to that of ^{56}Co decay, suggesting that during this phase γ-ray trapping was efficient. However, the steeper decay rate beyond day 310 indicates that either the supernova had become more transparent to γ-rays and γ-ray leakage was significant or dust formation occurred in the supernova ejecta, or it could be a consequence of both the phenomena.

A comparison of the light curves of SN 2004et with those of the well-studied SNe IIP, SN 1999em (Leonard et al. 2002a) and SN 1999gi (Leonard et al. 2002b) is made. The *UBVRI* light curves of SN 1999em and SN 1999gi, shifted by arbitrary units in magnitude

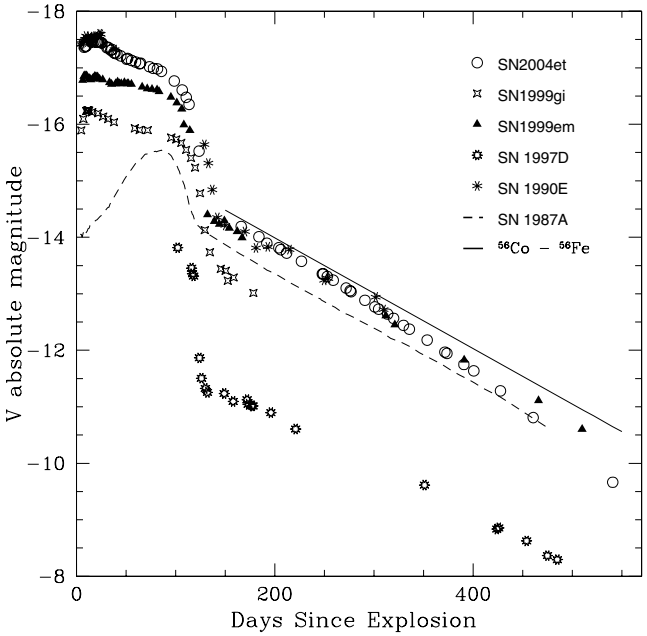

Figure 3. Absolute V light curve of SN 2004et along with those of other SNe IIP. The slope of ^{56}Co to ^{56}Fe radioactive decay is also shown.

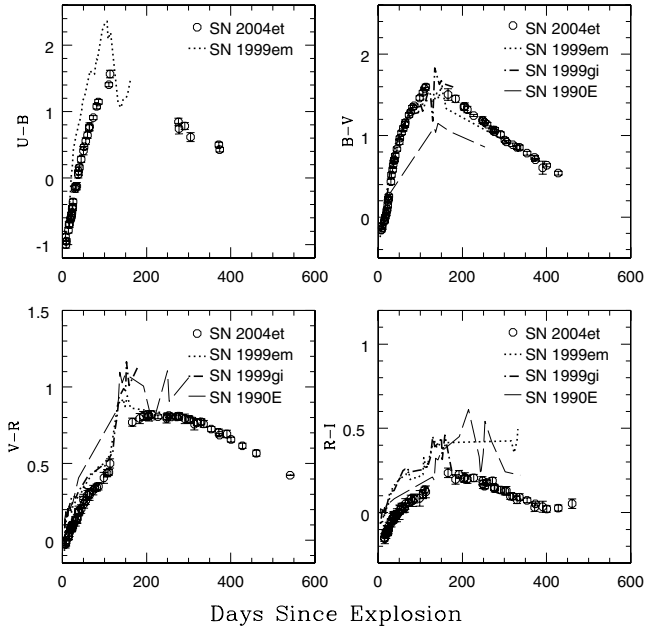

Figure 4. Colour curves of SN 2004et compared with other SNe IIP.

to match the respective light curves of SN 2004et, are also plotted in Fig. 2. The light curves of all the three SNe are remarkably similar during the early phases. The length of the plateau is also very similar, ∼100–120 d for all three events. However, the rate of decline during the nebular phase (beyond day 150) is different; SN 2004et has a steeper decline, indicating a probable difference in the fraction of γ-rays that escape through the supernovae ejecta. It may be noted that the late time photometry of the supernovae is affected significantly by the underlying background of the host, which may flatten the light curve. However, as SN 2004et occurred in the outskirts of the spiral arm, with probably no bright underlying region, background contamination in the late phase is expected to be low, but that may not be the case with SN 1999em and SN 1999gi.

In Fig. 3, we compare the absolute V light curve of SN 2004et with those of other SNe IIP, namely, SN 1999em (Hamuy et al. 2001; Leonard et al. 2002a; Elmhamdi et al. 2003b), SN 1999gi (Leonard et al. 2002b), SN 1997D (Benetti et al. 2001 and references therein), SN 1990E (Schmidt et al. 1993) and SN 1987A (Hamuy et al. 1988). The supernovae magnitudes have been corrected for extinction using the Cardelli, Clayton & Mathis (1989) extinction law and the following $E(B-V)$: 0.21 for SN 1999gi, 0.10 for SN 1999em, 0.00 for SN 1997D, 0.50 for SN 1990E and 0.15 for SN 1987A. A value of $E(B-V) = 0.41$ is used for SN 2004et (see Section 4). The distance used to calculate the absolute magnitudes and fluxes is 11.1 Mpc for SN 1999gi (Leonard et al. 2002b), 11.7 Mpc for SN 1999em (Leonard et al. 2003), 13.4 Mpc for SN 1997D (Benetti et al. 2001 and references therein), 21 Mpc for SN 1990E (Schmidt, Krishner & Eastman 1992) and 0.0468 Mpc for SN 1987A (Hamuy et al. 1988). A distance of 5.6 Mpc is used for SN 2004et (see Section 4). Distance estimates for SN 1990E and SN 1999gi are based on the expanding photosphere method (EPM), SN 1999em distance estimate is based on Cepheid variables (Leonard et al. 2003). For SN 1999em, Cepheid distance is nearly 50 per cent greater than the values derived using the EPM. The major source of discrepancy between the distances based on EPM and Cepheid may be attributed to the underestimate of the theoretically derived dilution factors used in EPM analysis; however, other sources of statistical and systematic uncertainty cannot be neglected.

The shape of the light curves of SN 2004et, SN 1999em and SN 1999gi is very similar, and the length of the plateau is also almost the same. The absolute magnitude of SN 2004et is similar to that of SN 1990E and is brighter than the other SNe IIP compared here. The average absolute V magnitude during the plateau phase, estimated by taking the unweighted mean of the magnitudes from 20 to 100 d after the explosion, is −17.14 for SN 2004et, −15.97 for SN 1999gi and −16.69 for SN 1999em.

The reddening-corrected $(U-B)$, $(B-V)$, $(V-R)$ and $(R-I)$ colour curves of SN 2004et are shown in Fig. 4. Also shown in the same figure, for comparison, are the respective colour curves of SN 1999em, SN 1999gi and SN 1990E. There is a notable difference in the colour evolution of SN 2004et with those of other SNe IIP in comparison. As noted by Li et al. (2005b), during the first month the $(U-B)$ and $(B-V)$ colours of SN 2004et evolve more slowly compared to SN 1999em, the same trend continues till ∼150 d since explosion. During this period, the overall colours of SN 2004et are bluer compared to the other SNe IIP. Beyond ∼200 d after explosion, the $(B-V)$ and $(V-R)$ colours of SN 2004et are similar to the other SNe IIP. The $(R-I)$ colour is bluer compared to SN 1999em even beyond day 200.

3 SPECTROSCOPY

3.1 Spectroscopic evolution

The spectroscopic evolution of SN 2004et in the rest frame of the SN is displayed in Figs 5 to 7. All the spectra have been Doppler corrected for the recession velocity of the host galaxy, taken as 45 km s^{-1} (Sandage & Tammann 1981). Our first spectrum corresponds to ∼25 d after explosion. The spectrum has a blue continuum with well-developed P Cygni profiles of hydrogen Balmer lines (up to Hϵ). The Hα line is emission dominated with a shallow P Cygni profile, which appears to consist of two components. The second, high-velocity absorption component is marked 'A' in Fig. 5. Apart

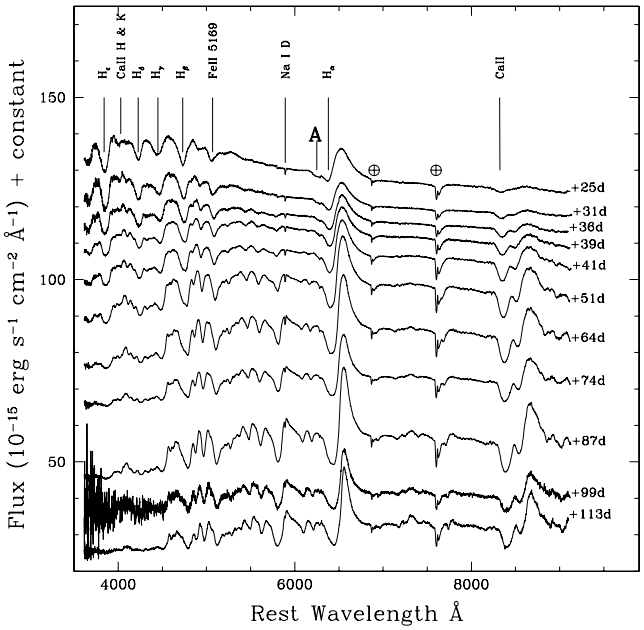

Figure 5. Spectral evolution of SN 2004et during plateau phase.

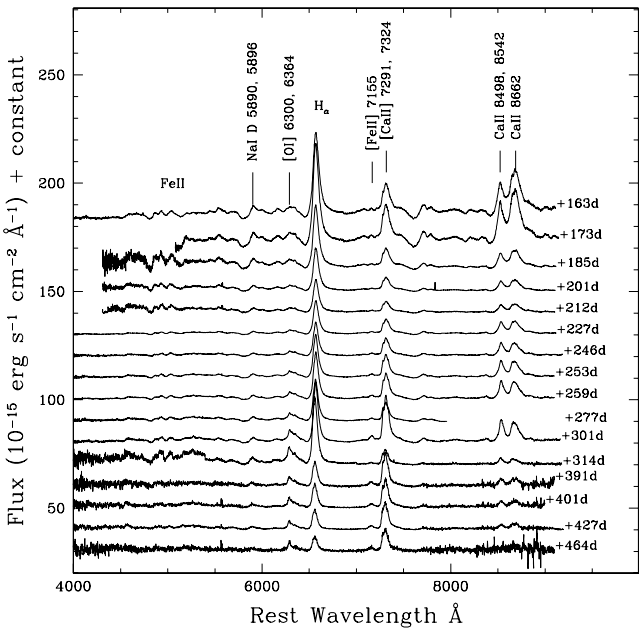

Figure 7. Spectral evolution of SN 2004et in the nebular phase.

from the hydrogen Balmer lines, Ca II (H & K) lines 3934, 3968 Å, Fe II 5169 Å and the Ca II infrared (IR) triplet 8498, 8542, 8662 Å are clearly seen in the spectrum. Interstellar Na I D absorption features at 5890, 5896 Å are also present. By day 39, Na I D absorption lines, Fe II lines 4924, 5018, 5535 Å, Sc II line 5527 Å and other blends of Fe II, Sc II, Ba II start appearing. Fig. 6 shows the spectrum taken 63 d after the explosion, with line identification following Leonard et al. (2002a). In the later phase, ∼74 d after explosion, except for Hα and Hβ, the Balmer lines are obscured by metal lines.

The two-component P Cygni profile of Hα noted by Li et al. (2005b) in a spectrum obtained 20 d after the explosion is clearly seen in our spectrum of day ∼25. This feature was present until ∼113 d, until the end of the plateau phase. This feature was also present in the spectrum of SN 1999em and has been identified as a high-velocity component of Hα (Leonard et al. 2002a). Similar high-velocity component features are noted in Hβ and Na I lines also. These high-velocity components could be arising due to the interaction of the supernova ejecta with the pre-supernova circumstellar material. Baron et al. (2000) interpret the double component P Cygni profiles as being produced by a combination of the usual wide P Cygni profile and a second P Cygni profile with a highly blueshifted absorption, corresponding to two line-forming regions in the expanding atmosphere of the supernova.

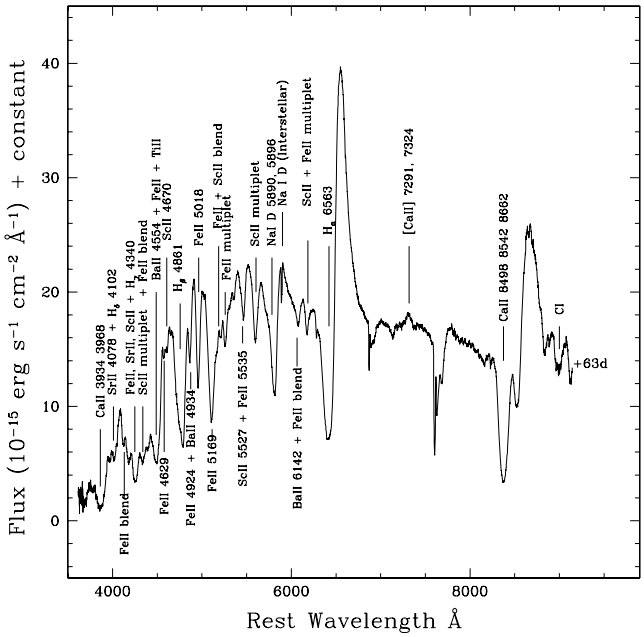

Figure 6. Spectral line identification in plateau phase.

As the supernova ages, the absorption components of Hα, Hβ and the Ca II IR triplet become narrower and deeper. In the blue region of the spectrum, numerous metal lines due to Fe, Sc, Ba and Sr appear, and the emission-line strength increases with time till the supernova enters into the nebular phase. The spectrum obtained ∼113 d after the explosion is still dominated by absorption features due to metal lines, indicating that the supernova had not yet entered into the nebular phase. However, forbidden lines due to oxygen [O I] 6300, 6364 Å, iron [Fe II] 7155 Å, calcium [Ca II] 7291, 7324 Å start appearing in the spectrum. The spectrum obtained ∼163 d after explosion (Fig. 7) shows a significant evolution compared to day 113. The spectrum is more emission dominated, featuring the onset of the nebular phase. In this spectrum, the Hα profile has narrowed down and the nebular emission lines of [O I] 6300, 6364 Å and [Ca II] 7291, 7324 Å are well developed.

In the spectra of day 391 (Fig. 7) and later, the [Ca II] 7291, 7324 Å line is strong compared to Hα, a feature noted in the spectrum of SN 1999em around the same epoch (Elmhamdi et al. 2003b), but not detected in the SNe IIP, SN 1990E (Benetti et al. 1994), SN 1997D (Benetti et al. 2001 and references therein) and SN 2003gd (Hendry et al. 2005). Fig. 8 shows the luminosity evolution of the nebular lines, Hα and [O I] 6300, 6364 Å for SN 2004et. Also shown in the same figure, for a comparison, are the corresponding luminosities for SN 1987A at similar epochs. The nebular line luminosities of SN 2004et before day 300 are similar to SN 1987A. Beyond day 400, SN 2004et lines have lower luminosities.

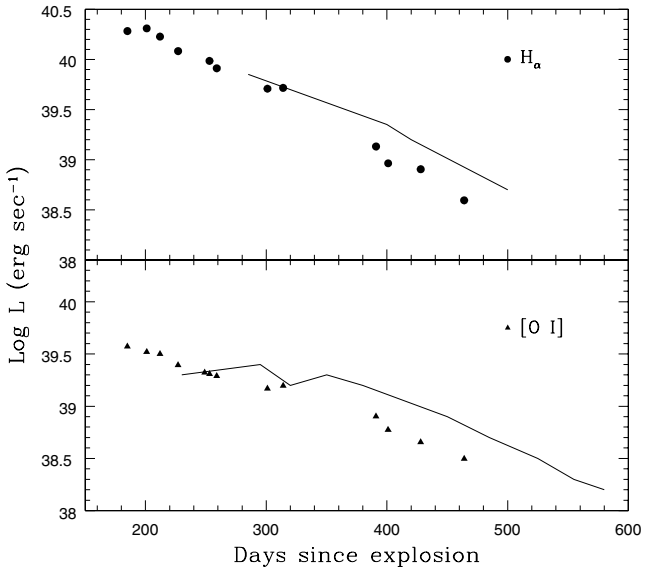

Figure 8. The temporal evolution of the luminosity of nebular lines Hα and [O I] for SN 2004et, overplotted curve corresponds to SN 1987A.

3.2 Expansion velocity of SN 2004et

The photospheric velocity of the ejecta can be estimated from the minimum of the absorption feature of weak, unblended lines. Hamuy et al. (2001) have shown that the use of Fe II (multiplet 42) at 4924, 5018, 5169 Å provides a good estimate of the photospheric velocity during the plateau phase. As the supernova ages, it becomes difficult to define the minimum of Fe II 5169 Å line, and hence the velocity measurement using this line is not a good estimate at these phases. The photospheric velocity estimated using these lines is plotted in Fig. 9. The velocity estimated using the Fe II 4924 Å line (Fig. 9) is lower due to the blending of this line with Ba II 4934 Å (Hendry et al. 2005).

Also plotted in Fig. 9 are the velocities determined using the absorption minima of Hα, Hβ and the high-velocity component of Hα.

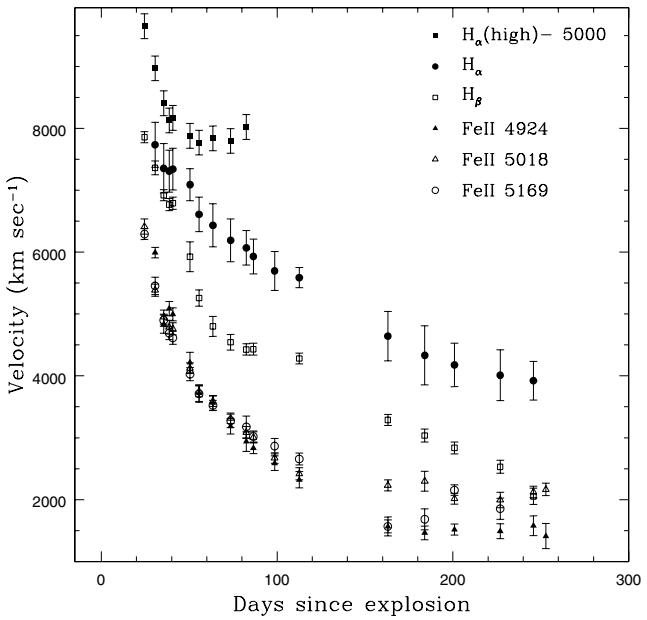

Figure 9. Velocity evolution of SN 2004et.

These velocity estimates are higher due to higher optical depths. The evolution of the high-velocity component of Hα is similar to that of normal component. A comparison of the photospheric expansion velocity determined for SN 2004et, using the weak unblended iron lines, with those of SN 1999em (Hamuy et al. 2001) and SN 1999gi (Leonard et al. 2002b) indicates that SN 2004et has a higher expansion velocity at similar epochs. For further analyses, we use the average photospheric velocity estimated using the weak iron lines.

4 REDDENING AND DISTANCE ESTIMATES

The interstellar Na lines are clearly seen in the spectra presented here. The equivalent width of the Na I D lines measured from the spectra presented here is 1.70 Å, which corresponds to a total reddening of $E(B-V) = 0.43$ mag, following the empirical relation by Barbon et al. (1990). This estimate is consistent with the estimate by Zwitter et al. (2004) based on equivalent widths of the Na I lines in a high-resolution spectrum. The Galactic reddening in the direction of NGC 6946 is $E(B-V) = 0.34$ mag (Schlegel, Finkbeiner & Davis 1998), which implies that the supernova has suffered minimal extinction in the host galaxy. We use $E(B-V) = 0.41$ (Zwitter et al. 2004) mag as the total reddening for further analysis.

The H I Tully–Fisher relation (Pierce 1994) indicates a distance of 5.5 Mpc to NGC 6946, while the CO Tully–Fisher relation (Schoniger & Sofue 1994) indicates a distance of 5.4 Mpc. The 'EPM' for the IIP supernova SN 1980K that occurred in NGC 6946 (Schmidt et al. 1994) yields a distance of 5.7 Mpc. Hamuy & Pinto (2002) have shown that the expansion velocities of the ejecta of SNe IIP are correlated with their bolometric luminosities during the plateau phase. Based on this correlation, they establish a 'standard candle method (SCM)' to estimate the distance to the supernovae. Nugent et al. (2006) proposed a refinement to the SCM method by introducing the use of $(V-I)$ colour during the plateau phase at day 50 to perform extinction correction rather than relying on colours at the end of the plateau. Using equation (1) of Nugent et al. (2006), with the fitting parameters for low-redshift SNe IIP and the observed expansion velocity at day 50 $v_{50} = 4122 \pm 170$ km sec^{-1}, we estimate the distance to SN 2004et as $5.7^{+0.3}_{-0.3}$ Mpc. Based on all the estimates, an average distance of 5.6 Mpc is assumed for SN 2004et.

5 *UBVRI* BOLOMETRIC LIGHT CURVE AND ^{56}NI MASS

5.1 *UBVRI* bolometric light curve

The *UBVRI* photometry presented in Section 2.3 is used to derive the *UBVRI* bolometric light curve of SN 2004et. The optical magnitudes have been corrected for reddening values mentioned in Section 2.3 using Cardelli et al. (1989) extinction law, the corrected magnitudes are then converted to fluxes according to Bessell, Castelli & Plez (1998). The *UBVRI* bolometric fluxes were derived by fitting a spline curve to the *U*, *B*, *V*, *R* and *I* fluxes and integrating it over the wavelength range 3200–10 600 Å, determined by the response of the filters used. There are some gaps in the *U*-band light curve specially after the plateau; the missing magnitudes were obtained by interpolation. In the later stage, however, the light curve is linearly extrapolated to get the missing magnitudes in the *U* band. No corrections have been applied for the missing fluxes in the ultraviolet and the near-IR region. Fig. 10 shows the *UBVRI* bolometric light curve of SN 2004et. Also plotted in the same figure are

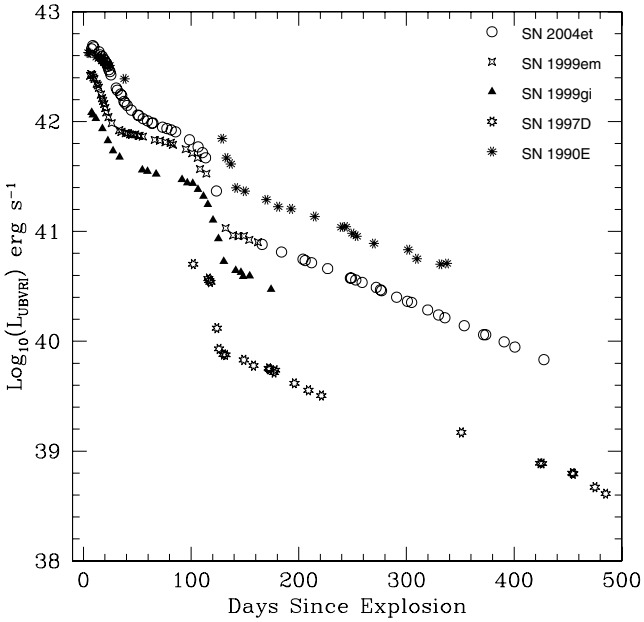

Figure 10. Comparison of *UBVRI* bolometric light curve of SN 2004et with those of other Type IIP SNe.

the *UBVRI* bolometric light curves of SN 1999em, SN 1999gi, SN 1997D and SN 1990E. The *UBVRI* bolometric light curve for SN 1990E is taken from the literature (Schmidt et al. 1993), while for other supernovae the *UBVRI* bolometric luminosities are derived from the photometry reported in the references cited in Section 2.3. Since no *U*-band magnitudes were available for SN 1999gi and SN1997D, the contribution of the *U* flux to the total *UBVRI* flux was assumed to be similar to SN 1999em and SN 2004et. A comparison of the *UBVRI* bolometric light curve of SN 2004et with the other SNe IIP indicates SN 2004et had a higher luminosity. The luminosity during the initial phases is very similar to SN 1990E but is considerably lower in the post-plateau decline.

5.2 ^{56}Ni mass

For most SNe IIP, the early (150–300 d) bolometric luminosity on the radioactive tail is equal to the luminosity of the radioactive decay of ^{56}Co. The mass of ^{56}Ni synthesized during the supernova explosion can thus be estimated from the late time bolometric light curve. In absence of IR photometry for SN 2004et, we followed Hamuy (2003) to estimate the tail bolometric luminosity L_t, using the *V* magnitudes during the nebular phase and a bolometric correction of 0.26 mag. The tail luminosity is then used to estimate the nickel mass using equation (2) in Hamuy (2003). Based on the luminosity of SN 2004et during 250–315 d, estimated using the *V* magnitudes, we estimate the ^{56}Ni mass to be $0.060 \pm 0.02\,M_\odot$.

Elmhamdi, Chugai & Danziger (2003a) find a correlation with the ^{56}Ni mass and the rate of decline in the *V*-band light curve from the plateau to the tail. The maximum gradient during the transition from plateau to nebular phase, defined by a steepness parameter $S = dM_V/dt$, is found to anticorrelate with ^{56}Ni mass, in the sense that the steeper the decline at the inflection, the lower is the ^{56}Ni mass. Using a sample of 10 SNe IIP, Elmhamdi et al. (2003a) derive the following relation:

$$\log\ M(^{56}\mathrm{Ni}) = -6.2295\ S - 0.8147. \quad (1)$$

An accurate determination of the steepness parameter *S* requires a well-sampled *V*-band light curve during the end of plateau to the beginning of the radioactive tail. Unfortunately, we do not have a very well sampled light curve during this phase. However, with the available points, we estimate the steepness parameter *S* as 0.062 ± 0.02. Using this, the mass of ^{56}Ni is found to be $0.062 \pm 0.02\,M_\odot$, which agrees very well with the ^{56}Ni mass derived from *V* magnitude on the radioactive tail.

The nickel mass may also be estimated comparing the bolometric light curve of SN 2004et with that of SN 1987A, assuming that the γ-ray deposition for SN 2004et is the same as that for SN 1987A. The tail bolometric luminosity of SN 2004et (∼250–300) is found to be ∼1.6 times fainter than that of SN 1987A. This implies a ^{56}Ni mass of $0.048 \pm 0.01\,M_\odot$ for SN 2004et, for a value of $0.075\,M_\odot$ for SN 1987A (Turatto et al. 1998 and references therein). This will be the lower limit of ^{56}Ni mass, as the bolometric curve for SN 2004et does not include contribution from near-IR region.

The mean nickel mass derived using the *V*-band magnitudes in the nebular phase and steepness parameter *S* is $0.06 \pm 0.02\,M_\odot$.

Chugai (1990) and Elmhamdi et al. (2003a) find that the Hα luminosity at the nebular phase can be used to estimate the nickel mass. The Hα luminosity is found to be proportional to ^{56}Ni mass during 200–400 d after the explosion. Comparing the Hα luminosity of SN 2004et around day 250 (Fig. 8, top panel) with that of SN 1987A during the same phase, it is found that the Hα luminosities in both SNe are similar. Assuming the mass, energy and mixing conditions do not vary strongly, this indicates the nickel mass in SN 2004et to be similar to that estimated for SN 1987A. This is consistent with the photometric estimates.

6 DUST FORMATION IN THE EJECTA

The formation of dust in the supernova ejecta increases the rate of decline of the optical, especially the *V*-band light curve, as the optical light is reprocessed by the dust and an excess emission in IR is observed. Further, dust formation in the inner envelope of the supernova ejecta shifts the peak of the optical and IR emission lines towards blue, due to a preferential extinction of the redshifted edge of the emission lines by the dust (Lucy et al. 1991). The signature of dust formation was seen in SN 1987A (Danziger et al. 1991) and SN 1999em (Elmhamdi et al. 2003b) as an observable blueshift in the emission peaks of the [O I] doublet components, beyond ∼400 d. It should be noted that both SNe showed an early blueshift (∼200–300 d) in the [O I] component, probably as a result of superposition of the blend of Fe II lines (multiplet 74).

Fig. 11 shows the temporal evolution of the Hα and [O I] 6300, 6364 Å line profiles during 277–465 d. A blueshift in the emission peak is clearly seen beyond day 300 in both lines. Further, the Hα line shows a clear flattening of the emission peak. The blueshift in the emission peak and the flattening were seen in both SN 1987A and SN 1999em during the dust formation epoch. The absence of any 'blue bump' in the [O I] line due to Fe II 6250 Å feature (Fig. 11, top panel) indicates that the observed blueshift in the emission peak is not due to a blending of Fe II lines, and more likely due to dust formation.

It is evident from Fig. 3 that the decline rate of the light curve of SN 2004et in the *V* band starts steepening ∼320 d after the explosion. A similar effect was seen in both SN 1987A and SN 1999em during dust formation. It should, however, be noted here that dust formation occurred at much later phases, beyond day 400 in both these SNe.

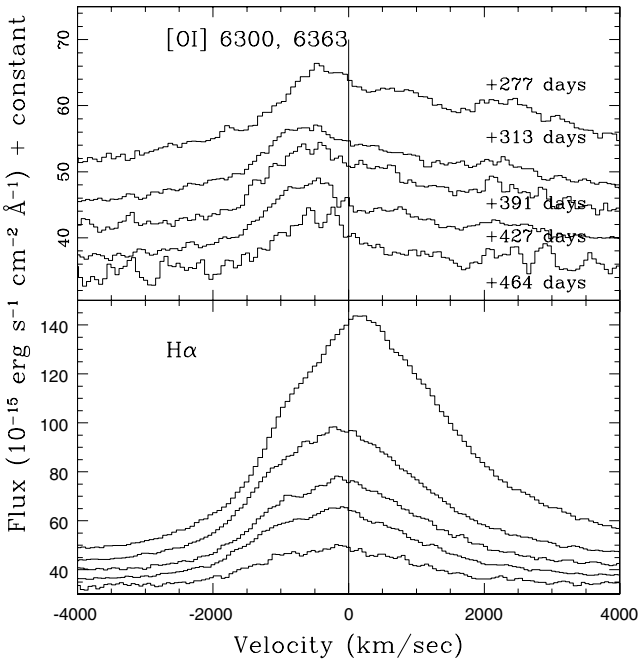

Figure 11. Temporal evolution of line profile of oxygen doublet [O I] 6300, 6364 Å (top panel) and Hα (bottom panel). The vertical line corresponds to the zero velocity of the [O I] 6300 Å and Hα. The epochs are as marked for the [O I] profile.

The evolution of the emission-line profiles together with the steeping of the light curve beyond day ∼320 suggests an early dust formation in the case of SN 2004et.

7 PROGENITOR STAR PROPERTIES

The supernova outburst properties depend on three basic parameters: the mass M of the envelope that is ejected, the radius R of the star prior to the outburst and the energy E of explosion. An analysis of supernova light curve combined with the spectroscopic evolution allows the derivation of these important parameters. With the help of hydrodynamic models of SNe IIP, Litvinova & Nadyozhin (1985) derived expressions for these parameters in terms of the observable parameters, namely, the length of the plateau Δt, the absolute magnitude M_V at the midpoint of the plateau and the velocity of photosphere $U_{\rm ph}$ at mid plateau.

The light curve of SN 2004et indicates the length of the plateau to be $\Delta t = 120 \pm 10$ d. The absolute magnitude at mid-plateau is $M_V = -17.14$ mag. The weak iron lines indicate a mid-plateau velocity $U_{\rm ph} = 3560 \pm 100\,{\rm km\,s^{-1}}$. Using these values and the relations given by Litvinova & Nadyozhin (1985), we estimate the explosion energy $E_{\rm exp} = 1.20^{+0.4}_{-0.3} \times 10^{51}$ erg.

The luminosity of [O I] doublet ∼1 yr after the explosion is powered by the γ-ray deposition and by ultraviolet emission arising from the deposition of γ-rays in oxygen-poor material. The [O I] doublet luminosity is related to the mass of oxygen, the 'excited' mass in which the bulk of the radioactive energy is deposited and the efficiency of transformation of the energy deposited in oxygen into the [O I] luminosity. The [O I] luminosity in SN 1987A implies an oxygen mass in the range 1.5–2 $M_\odot$. The fact that derived [O I] luminosity for SN 2004et before dust formation is comparable to that of SN 1987A at similar epochs implies similar oxygen mass in SN 2004et also. The nucleosynthesis computations (Chugai 1994; Woosley & Weaver 1995) indicate that this oxygen mass corresponds to a main-sequence stellar mass of 20 $M_\odot$. An analysis of the radio light curve of SN 2004et by Chevalier, Fransson & Nymark (2006) indicates a mass-loss rate for the progenitor that suggests a mass of 20 $M_\odot$, similar to the estimate based on a comparison of the [O I] luminosity with that of SN 1987A. However, Li et al. (2005b) estimate the progenitor mass to be ∼15 $M_\odot$ and also the progenitor to be a yellow supergiant.

8 SUMMARY

We have presented *UBVRI* photometric and spectroscopic data for SN 2004et from ∼8 to ∼541 d after the explosion. The shape of the light curve, as well as the spectral evolution, indicates that it is Type IIP supernova, which was caught young, soon after the shock breakout. SN 2004et reached maximum in *B* band on JD 245 3280.90, ∼10 d after the explosion. The luminosity at maximum indicates SN 2004et to be at the brighter end of SNe IIP. The late-phase photometry indicates that the decline rate of light curve during ∼180–300 d was similar to the ^{56}Co to ^{56}Fe radioactive decay, while it was significantly faster beyond ∼320 d.

The spectra of SN 2004et in early phase show an Hα profile that is emission dominated with P Cygni profile that is shallower than other SNe IIP. The velocity evolution of SN 2004et determined using the weak iron lines is similar to other well-studied SNe IIP, although the photospheric velocity in SN 2004et was higher than other SNe IIP at all epochs. The Hα line indicates the presence of a high-velocity component in the early phases, with the velocity of this component being ∼7000 km s^{-1} higher than the normal component.

The mass of ^{56}Ni synthesized during the explosion is estimated to be $0.06 \pm 0.02\,M_\odot$.

The Hα and [O I] 6300, 6364 Å line profile evolution beyond day 320, and the steepening of the *V* light curve at the same epoch, is interpreted as an effect of an early dust formation.

The brightness of the plateau, its duration and the expansion velocity of the supernova at the middle of the plateau are used to estimate the explosion energy $E_{\rm exp} = 1.20^{+0.38}_{-0.30} \times 10^{51}$ erg. The main-sequence mass of the progenitor based on [O I] luminosity is estimated to be 20 $M_\odot$.

ACKNOWLEDGMENTS

We thank the anonymous referee for useful comments, which helped in improving the manuscript. We thank all the observers of the 2-m HCT who kindly provided part of their observing time for the supernova observations. We also thank Jessy Jose and S. Ramya for their help during observations. This work has made use of the NASA Astrophysics Data System and the NASA/IPAC Extragalactic Data base (NED) which is operated by Jet Propulsion Laboratory, California Institute of Technology, under contract with the National Aeronautics and Space Administration.

REFERENCES

Barbon R., Benetti S., Rosino L., Cappellaro E., Turatto M., 1990, A&A, 237, 79
Baron R., Ciatti F., Rosino L., 1979, A&A, 72, 287
Baron E. et al., 2000, ApJ, 545, 444
Benetti S., Cappellaro E., Turatto M., Della Valle M., Mazzali P., Gouiffes C., 1994, A&A, 285, 147
Benetti S. et al., 2001, MNRAS, 322, 361
Bessell M. S., 1990, PASP, 102, 1181

Bessell M. S., Castelli F., Plez B., 1998, A&A, 333, 231
Cardelli J. A., Clayton G. C., Mathis J. S., 1989, ApJ, 345, 245
Chevalier R. A., Fransson C., Nymark T. K., 2006, ApJ, 641, 1029
Chugai N. N., 1990, SvA Lett., 16, 457
Chugai N. N., 1994, ApJ, 428, L17
Danziger I. J., Lucy L. B., Bouchet P., Gouiffes C., 1991 in Woosley S. E., ed., Supernovae. Springer, New York, p. 69
Elmhamdi A., Chugai N. N., Danziger I. J., 2003a, A&A, 404, 1077
Elmhamdi A. et al., 2003b, MNRAS, 338, 939
Filippenko A. V., Foley R. J., Treu T., Malkan M. A., 2004, IAU Circ., 8414
Hamuy M., 2003, ApJ, 582, 905
Hamuy M., Pinto P. A., 2002, ApJ, 566, L63
Hamuy M., Suntzeff N. B., Gonzalez R., Martin G., 1988, AJ, 95, 63
Hamuy M. et al., 2001, ApJ, 558, 615
Hendry M. A. et al., 2005, MNRAS, 359, 906
Landolt A. U., 1992, AJ, 104, 340
Leonard D. C. et al., 2002a, PASP, 114, 35
Leonard D. C. et al., 2002b, AJ, 124, 2490
Leonard D. C., Kanbur S. M., Ngeow C. C., Tanvir N. R., 2003, ApJ, 594, 247
Litvinova Y., Nadyozhin D. K., 1985, SvA Lett., 11, 45
Li W., Filippenko A. V., Van Dyk S. D., 2005a, Astronomer's Telegram (ATel), 492
Li Weidong, Van Dyk S. D., Filippenko A. V., Cuillandre J.-C., 2005b, PASP, 117, 121
Li Weidong, Van Dyk S. D., Filippenko A. V., Cuillandre J., Jha S., Bloom J. S., Riess A. G., Livio M., 2006, ApJ, 641, 1060
Lucy L. B., Danziger I. J., Gouiffes C., Bouchet P., 1991, in Woosley S. E., ed., Supernovae. Springer, New York, p. 82
Nugent P. et al., 2006, ApJ, 645, 841
Patat F., Baron R., Cappallaro E., Turatto M., 1994, A&A, 282, 731
Pierce M. J., 1994, ApJ, 430, 53
Sandage A., Tammann G. A., 1981, Revised Shapley-Ames Catalog of Bright Galaxies. Carnegie Inst. Washington
Schlegel D. J., Finkbeiner D. P., Davis M., 1998, ApJ, 500, 525
Schmidt B. P., Krishner R. P., Eastman R. G., 1992, ApJ, 395, 366
Schmidt B. P. et al., 1993, AJ, 105, 2236
Schmidt B. P., Krishner R. P., Eastman R. G., Phillips M. M., Suntzeff N. B., Hamuy M., Maza J., Aviles R., 1994, ApJ, 432, 42
Schoniger F., Sofue Y., 1994, A&A, 283, 21
Smartt S. J., Maund J. R., Hendry M. A., Tout C. A., Gilmore G. F., Mattila S., Benn C. R., 2004, Sci, 303, 499
Stockdale C. J., Weiler K. W., Van Dyk S. D., Sramek R. A., Panagia N., Marcaide J. M., 2004, IAU Circ., 8415
Turatto M. et al., 1998, ApJ, 498, L129
Van Dyk S. D., Li W., Filippenko A. V., 2003, PASP, 115, 1289
Woosley S. E., Weaver T. A., 1995, ApJS, 101, 181
Zwitter T., Munari U., Moretti S., 2004, IAU Circ., 8413, 1

This paper has been typeset from a TEX/LATEX file prepared by the author.